ELSEVIER

Journal of Nuclear Materials 241–243 (1997) 1210–1216

journal of nuclear materials

Performance of beryllium, carbon, and tungsten under intense thermal fluxes

J. Linke [a,*], M. Akiba [b], H. Bolt [a], G. Breitbach [a], R. Duwe [a], A. Makhankov [c], I. Ovchinnikov [c], M. Rödig [a], E. Wallura [a]

[a] *Forschungszentrum Jülich GmbH, Association KFA-EURATOM, D-52425 Jülich, Germany*
[b] *Japan Atomic Energy Research Institute, Naka, Ibaraki 311-01, Japan*
[c] *D.V. Efremov Institute, St. Petersburg 189 631, Russia*

Abstract

Transient heat loads on a millisecond timescale with deposited energy densities beyond 1 MJ m^{-2} have been simulated in a plasma accelerator facility (VIKA) and in two high power electron beam teststands (JUDITH, JEBIS). Main objective of these experiments was to study and to compare the behaviour of different plasma facing materials (Be, CFC, W) under heat loads which occur during disruptions in future thermonuclear fusion reactors such as ITER. In these tests special attention was paid to the thermal shock resistance, the processes during melt layer formation, and the resulting material erosion. To perform these tests specific loading techniques and diagnostics have been developed and applied. Among these are high heat flux loading experiments at elevated temperatures ($T >$ DBTT) of the test coupons, fast surface pyrometry, and reliable techniques for the quantification of the absorbed energy.

Keywords: Energy deposition; Low-Z wall material; High-Z wall material; Erosion and particle deposition; Disruptions

1. Introduction

High heat flux experiments are an essential tool to evaluate the performance of plasma facing materials (PFM) under severe thermal loads. To evaluate the performance of ITER relevant PFM (Be-, CFC-, W-alloys) under disruption conditions, transient heat load experiments with deposited energy densities beyond 1 MJ m^{-2} on a millisecond timescale have been performed in a plasma accelerator facility (VIKA, D.V. Efremov Institute) and in two electron beam teststands (JUDITH, KFA; JEBIS, JAERI). Main objective of these tests was to quantify the thermal shock resistance, the resulting material erosion, and to analyze the processes during melt layer formation. Beside the investigation of the phenomena taking place during transient heat flux loading, great emphasis was laid on the assessment of grade specific aspects, i.e. the screening for a variety of PFMs with different material composition, different production techniques, and test specimens produced by different manufacturers.

2. Experimental procedure

The thermal load experiments have been performed in three test facilities capable to produce energetic heat flux pulses of a few milliseconds or less. VIKA is a coaxial plasma gun which can deliver plasma pulses of about 60–400 μs. The accelerated plasma is characterized by a strongly directed flow of particles (primarily hydrogen) with a low thermal energy of a few eV and a high velocity of plasma particles of $(0.5–1) \times 10^5$ m s^{-1}; the diameter of the loaded area has been determined by calorimetric measurements and is in the order of 15 mm full width at

* Corresponding author. Tel.: +49-2461 61 3230; fax: +49-2461 61 3699; e-mail: j.linke@kfa-juelich.de.

PII S0022-3115(96)00701-5

half maximum (FWHM) [1]. JUDITH and JEBIS are high heat flux (HHF) teststands which produce beams with electron energies up to 150 and 100 keV, respectively. In JUDITH [2] the electron beam which is generated in a W-cathode and focussed by magnetic lenses is scanned with a frequency up to 100 kHz over an area of typically 5×5 mm^2. In JEBIS [3] the electron beam is extracted from a plasma source; here the beam shows a characteristic Gaussian profile with typically 5–10 mm in diameter (FWHM). The maximum power densities in the two electron beam facilities are 15 and 2 GW m^{-2} with pulse durations of 1 ms or longer.

VIKA and JEBIS have been provided with heated sample holders which allow thermal shock tests at elevated temperatures (up to 1100°C); the energy absorbed by the test specimen is quantified by calorimetric methods. A special inner containment which has been installed in the JUDITH facility allows the HHF testing of beryllium [4]. In addition to calorimetric measurements in JUDITH the beam current absorbed by the test specimens can be measured directly; a fast pyrometer allows surface temperature measurements with a time resolution of better than 10 μs. Additional diagnostics which have been applied in the three test facilities are thermocouples, high speed video systems, and residual gas analysis.

Test samples investigated so far were different grades of commercial beryllium (S65C, TShG-200, TPG-56, TR-30), pyrolytic and fine grain graphite (EK98), Ti-doped graphite (RGTi), different carbon–carbon composites (e.g. A05, SEP N112, CX2002, MFC1) and tungsten. Typical sample geometries were $25 \times 25 \times 10$ mm^3, for tests in JUDITH with a loaded area of only 5×5 mm^2 also smaller test coupons ($12 \times 12 \times 5$ mm^3) have been used in order to get a higher resolution in weight loss measurements. The beryllium samples have been machined by spark erosion techniques which provide a rather smooth surface; most of the samples were polished after mechanical machining to guarantee a well defined surface for erosion measurements by laser-optical profilometric methods. In addition, material erosion was determined by weight

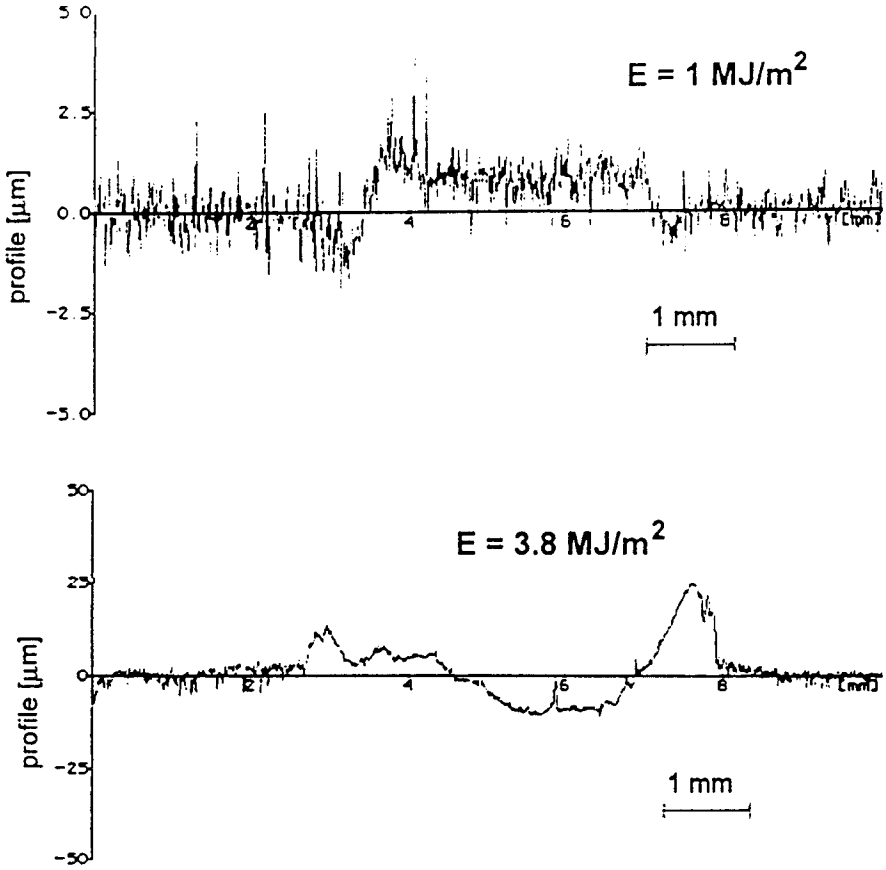

Fig. 1. Surface profilometry for two samples of beryllium S65C loaded in JUDITH at energy densities of 1.0 and 3.8 MJ m^{-2}, pulse duration 5 ms.

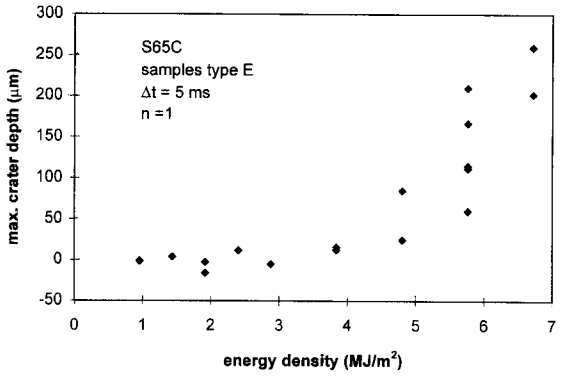

Fig. 2. Erosion behaviour of beryllium S65C in electron beam tests at pulse durations of 5 ms (single shot loading).

loss measurements; post irradiation analysis includes methods such as scanning electron microscopy (SEM), optical and quantitative metallography.

3. Results

3.1. Beryllium

To determine the threshold value for material damage a test series with stepwise increasing heat loads at a constant pulse duration (5 ms) has been performed on different beryllium grades. Fig. 1 shows surface profiles from the heat affected zone of beryllium S65C for incident energy densities of 1.0 and 3.8 MJ m^{-2} (for low-Z materials such as Be energy losses due to backscattered electrons are less than 10%). Up to energy densities of 1.4 MJ m^{-2} no surface modifications can be detected by SEM [5]; even machining groves are still visible after loading. Nevertheless, the surface profile shows a clear increase of the surface level by 1–2 μm. This swelling effect becomes more pronounced for increased energy densities; for 2.4 MJ m^{-2} a melting rim appears and for 2.9 MJ m^{-2} a first crater formation can be detected. Further increase of the electron beam current results in a marked dynamic melting process, and finally beyond 5.8 MJ m^{-2} whirling of the

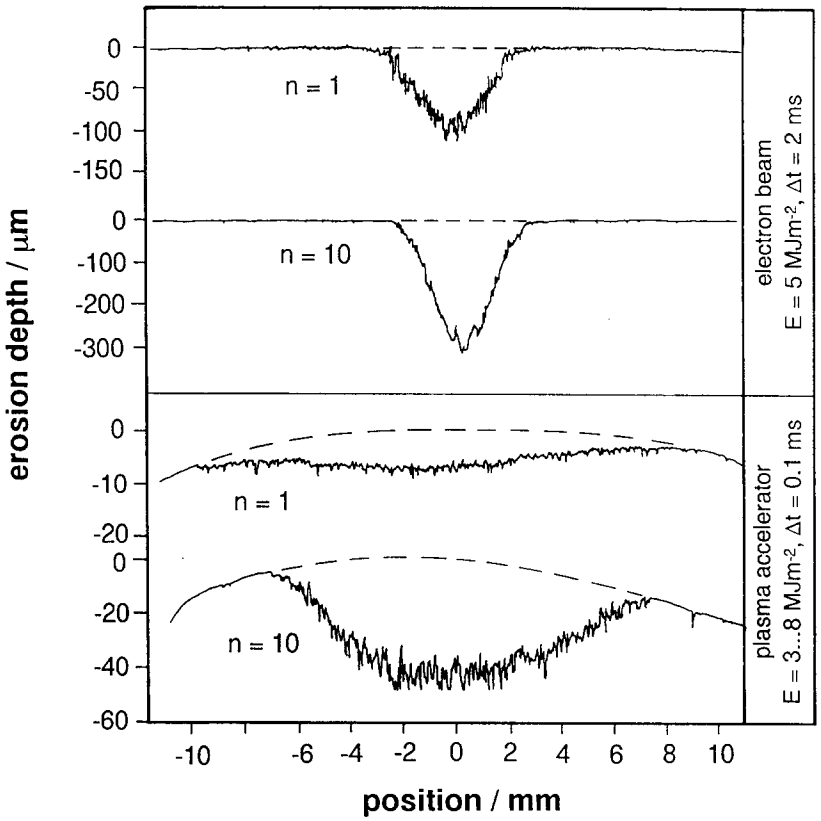

Fig. 3. Surface profilometry test specimens made from fine grain graphite EK98. Single ($n = 1$) and multiple shot loading ($n = 10$) in JEBIS and VIKA. The given energy densities are absorbed values determined by calorimetry.

molten material and droplet formation is becoming essential. Under these conditions a significant erosion process and sample weight loss can be measured. For beryllium grade S65C this effect (maximum crater depth versus deposited energy density) is shown in Fig. 2; for energy densities ≥ 5 MJ m^{-2} convective motion and removal of the melt layer results in a significant increase in crater depth. Beside material erosion the formation of disabling cracks has significant influence on the performance of beryllium as PFM in future fusion devices. Due to a reduced thermal shock resistance a more pronounced crack formation and even higher erosion rates have been determined. In general a repeated electron beam loading at energy densities below 3 MJ m^{-2} does not result in a progressive increase of the erosion depth and crack formation; this is not true for Be-grades with poor thermal shock resistance (e.g. TR-30). Detailed data from further high heat flux experiments on Be-grades are published elsewhere [5].

3.2. Carbon

Surface profiles from carbon samples loaded at identical energy densities do not show the above mentioned effects; this is mainly due to the fact that carbon is less ductile at elevated temperatures and due to the lack of a liquid phase. Fig. 3 shows erosion profiles for a fine grain graphite EK98 at incident energy densities of approximately 5 MJ m^{-2} for single ($n = 1$) and multiple shot loading ($n = 10$). These tests have been performed both in an electron beam (JEBIS) and a plasma accelerator test facility (VIKA). In all cases the erosion profile matches the Gaussian beam profile; redeposition of eroded material at the crater rim is not detectable. Both experiments, JEBIS and VIKA, show a strong effect on the pulse number: for the applied pulse duration of 2 ms a single shot electron beam pulse produces a crater with a depth of approximately 100 μm; 10 repeated pulses of identical energy density result in an increase in erosion depth of only a factor 3. A very similar effect can be observed for VIKA tests. The shape of the erosion craters is strongly influenced by the beam profiles. Independent from the beam profiles in VIKA the absolute erosion values are significantly (roughly a factor 10) smaller if compared with electron beam loading tests; this is mainly due to the vapor shielding effect which does not play any significant role in electron beam simulations because of the high electron energy [6,7].

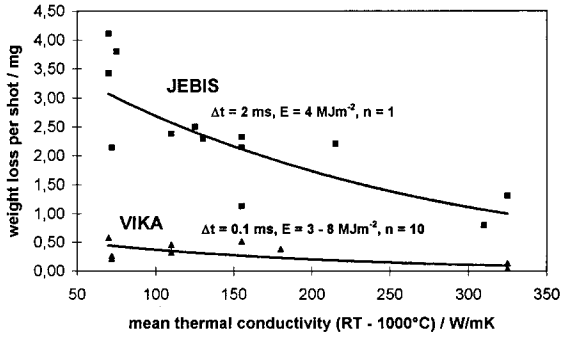

Fig. 4. Mean erosion weight loss per shot for different carbon materials plotted versus mean thermal conductivity of the test samples for a temperature range from RT to 1000°C.

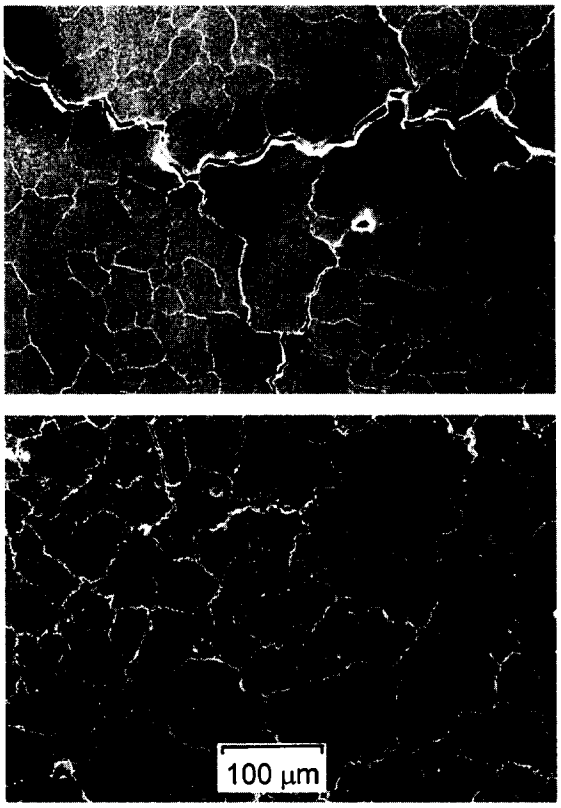

Fig. 5. Disruption simulation experiments on tungsten in the VIKA facility at elevated specimen temperatures (top: 320°C; bottom: 640°C); incident energy density: 7.5 MJ m^{-2}, pulse duration: 360 μs, number of pulses: 10.

The erosion of carbon materials depends strongly on the thermal conductivity of the applied graphites or CFC-materials. In Fig. 4 the erosion weight loss per shot for different grades is plotted versus the mean thermal conductivity of the test coupons parallel to the incident electron beam. For both types of experiments the resulting material erosion decreases drastically with increasing thermal conductivity, i.e. conduction of energy into the bulk of the PFM is becoming essential. Similar to the erosion data shown in Fig. 3, the weight losses of the plasma accelerator samples are significantly smaller (if normalized to the actual beam diameters these differences become more pronounced). Graphites with high coefficients of thermal

expansion (CTE) show a higher tendency to form thermally induced cracks; in general this effect has only little influence on fibre reinforced carbon materials.

3.3. Tungsten

The most significant damage to tungsten test samples in thermal shock tests in plasma accelerators or electron beam facilities is the formation of intergranular cracks, primarily perpendicular to the sample surface. These cracks tend to grow during repeated loading of the PFM. This crack formation effect was only observed on test samples which were loaded at room temperature. The service temperature of plasma facing components, however, will be in the order of several hundred degrees Celsius, depending on the prevailing design and HHF conditions. To investigate the effect of increased wall temperatures both in VIKA and JEBIS test samples have been exposed to severe thermal shocks at elevated sample temperatures (up to 1130°C). Fig. 5 shows SEM micrographs from tungsten surfaces loaded at 7.5 MJ m^{-2} (pulse duration: 360 μs, number of pulses: $n = 10$); the surface temperatures before loading were 320 and 640°C, respectively. The latter sample (as well as test coupons loaded at 450°C and above) only show a widening of the grain boundaries which is mainly due to plastic deformation during pulsed loading. Below a sample temperature of 450°C, which corresponds to the ductile-to-brittle-transition-temperature (DBTT) significant intergranular crack formation has been detected. Metallographic sections from these samples demonstrate cracks with a maximum depth of 1 mm. This effect is not specific for tungsten; this ductile behaviour at elevated temperatures is also expected for Be.

3.4. Beam current measurement

To provide a time resolved signal of the absorbed electrical current during electron beam loading, a current measurement has been established in JUDITH. The test coupons are grounded via a resistor (48 Ω) and the resulting voltage drop is measured. This signal is plotted in Fig. 6a for graphite EK98 loaded at pulses of 5 ms duration; the incident beam current has been varied in a range from 120 to 280 mA. The bottom curve (I_{inc} = 120 mA) shows an almost constant absorbed current of approximately 110 mA for the first 3 ms of the electron beam

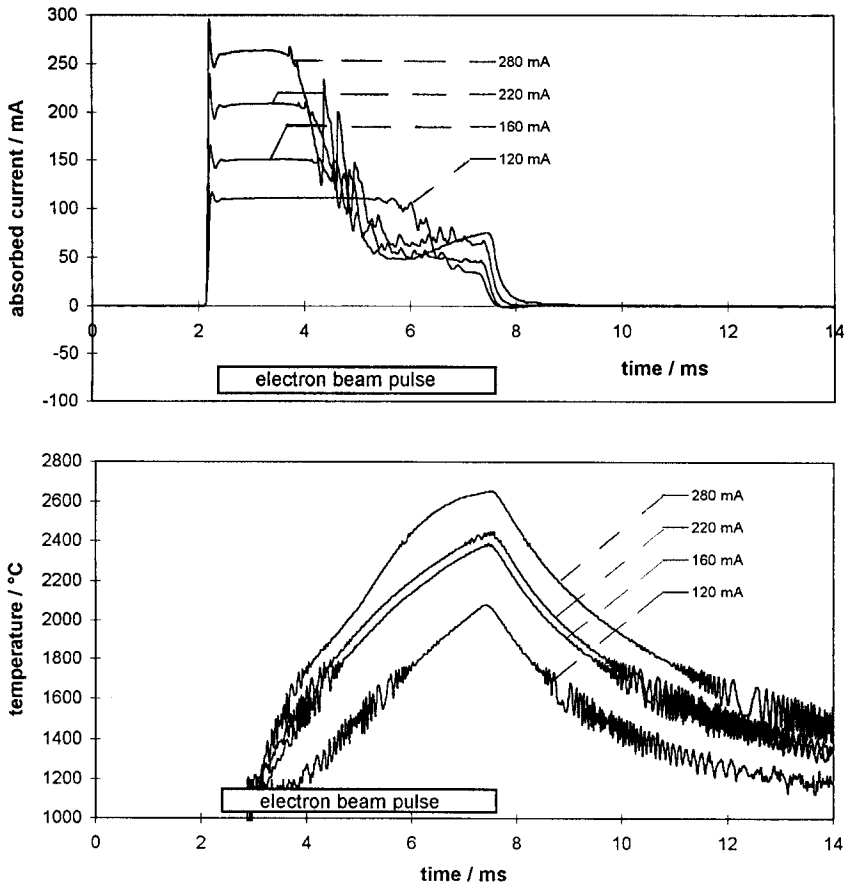

Fig. 6. Absorbed current and surface temperature during electron beam tests on fine grain graphite EK98 in JUDITH; pulse duration: 5 ms.

pulse; during the last 2 ms the net absorbed current drops to zero, however, the energy deposition remains almost unchanged during the full 5 ms electron beam pulse. This effect is associated with the emission of electrons (thermionic emission); in addition the release of charged particles from the heated surface (carbon clusters or grains) has been observed. In tokamaks these emission processes are leading to carbon blooms. Due to the strong temperature dependance the emission process should start earlier when higher heat fluxes are applied: With increasing beam currents the emission process starts after 2.0 ms for $I_{inc} = 160$ mA (1.7 and 1.4 ms for $I_{inc} = 220$ and 280 mA, respectively). Fig. 6b shows the corresponding surface temperatures measured by a specially developed high speed pyrometer; the sensitivity of this system is limited to temperatures ≥ 1100°C. This pyrometer has been calibrated under steady state conditions using electron beam heated graphite samples which were temperature controlled by a thermocouple and/or a two-colour-pyrometer. According to this calibration the emission process is becoming essential at surface temperatures of 1600 to 1700°C. A strong particle emission can be observed by video or photographic methods during electron beam loading of carbon materials in JUDITH. In previous experiments using long pulse electron beam heating (1.5 s) [8] strong particle emission has been observed above approximately $T = 2500$ K.

The intensity of this emission process decreases during the first few shots on a fresh polished graphite or CFC sample. This can be observed directly with the naked eye; on the other hand the decrease of the absorbed current is retarded with increasing pulse number. This effect is demonstrated in Fig. 7 which shows absorbed beam currents of graphite EK98 for single ($n = 1$) and multiple shot tests ($n = 2$, $n = 5$). In other words, a polished graphite surface is rather sensitive to particle erosion. According to SEM micrographs it is primarily the binder which is eroded first; in a second step graphite grains or grain fragments which remain only loosely bound can be eroded easily. After a conditioning phase of approximately 5 to 10 shots the erosion process remains constant. These findings are in good agreement with Fig. 3 where the most significant erosion took place in the first pulse. Due to local inhomogeneities in the graphites and CFCs, weight loss measurements on carbon materials in general show a large spreading (cf. Fig. 4).

Fig. 7 also shows current measurements for tungsten samples loaded with identical parameters of the JUDITH teststand. Here the absorbed current is significantly smaller due to the large fraction of backscattered electrons (approximately 50%). However, there is almost no current drop for identical absorbed currents (e.g. if compared with the 160 mA curve in Fig. 6). Surface temperature measurements on tungsten samples have not been performed because of the unknown emissivity. However, due to the higher thermal conductivity of W in comparison to graphite EK98 the tungsten surfaces remain colder. Since the electronic work function shows similar values for carbon and tungsten, it can be concluded that thermionic emission from the tungsten samples does not play any important role under the conditions reported in this paper [9]. Repeated shots have only little influence on the level of the absorbed current. Qualitatively beryllium and tungsten show a very similar behaviour.

4. Summary

A broad selection of different PFM for ITER based on beryllium, carbon, and tungsten has been investigated with respect to their behaviour under intense heat loads associated with severe disruptions. To simulate the damaging process, to evaluate the material performance and to select materials from a broad spectrum of commercially available grades, HHF experiments have been performed in a plasma accelerator and in two electron beam test facilities:

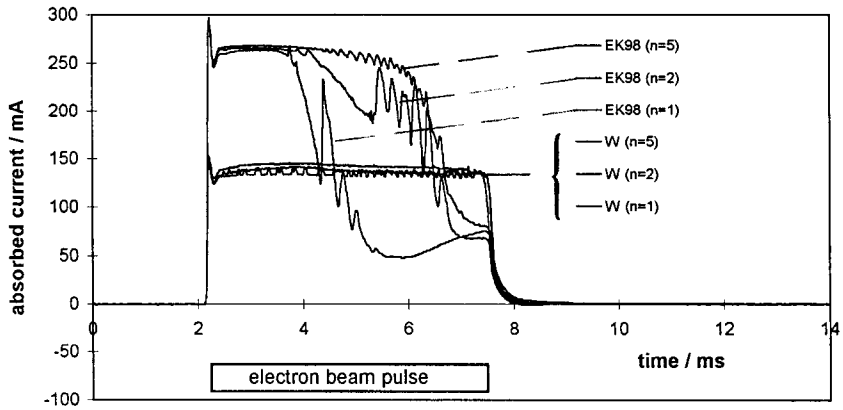

Fig. 7. Absorbed current during electron beam experiments on graphite EK98 and tungsten (incident current: 280 mA, pulse duration: 5 ms). The parameter n indicates the pulse number.

Beryllium shows first melting effects in electron beam tests (pulse duration = 5 ms) at 2.4 MJ m^{-2}; below this value swelling of the heat affected area has been observed. Droplet formation and increased material loss occurs above approximately 5 MJ m^{-2}. Grades with a high BeO content show increased crack formation and higher erosion losses.

The erosion of *carbon* based materials shows a strong dependance on the thermal conductivity perpendicular to the sample surface. The erosion process is associated with the emission of electrons and particles; this effect dominates during the first few heat pulses. Measurements of the absorbed current during electron beam loading shows a clear correlation with the emission process.

Tungsten shows a tendency to form deep intergranular cracks when loaded at temperatures below DBTT. HHF experiments performed at elevated temperatures do not show any disabling crack formation; under these conditions plastic deformation occurs in the heat affected surface layer.

References

[1] H. Bolt, V. Barabash, A. Gervash, J. Linke, H. Nickel, I. Ovchinnikov and M. Rödig, Fusion Eng. Des. 30 (1995) 225–232.

[2] R. Duwe, W. Kühnlein and H. Münstermann, Proc. 18th Symp. on Fusion Technology (SOFT), Karlsruhe, 22–26 August 1994, pp. 355–358.

[3] J. Linke, M. Akiba and I. Mazul, in: Thermal Shock and Thermal Fatigue Behavior of Advanced Ceramics, eds. G.A. Schneider and G. Petzow (Kluwer Academic Publishers, Dordrecht, 1993) pp. 343–354.

[4] J. Linke, R. Duwe, A. Gervash, W. Kühnlein, K. Nakamura, A. Peacock and M. Rödig, Proc. 2nd IEA Int. Workshop on Beryllium Technolgy for Fusion, INEL-report CONF-9509218 (1995) pp. 122–130.

[5] M. Rödig, R. Duwe, A. Gervash, J. Linke and A. Schuster, Proc. of the 7th Int. Workshop on Carbon Materials, Stockholm, 1995, Phys. Scr. Vol. T 4 (1996) 60.

[6] P.D. Rockett, J.A. Hunter, J.M. Gahl, J.T. Bradley III and R.T. Peterson, J. Nucl. Mater. 212–215 (1994) 1278–1282.

[7] A. Hassanein and I. Konkaskbaev, in: Atomic and Plasma–Material Interaction Data for Fusion, Vol. 5 (IAEA, Vienna, 1994) pp. 193–224.

[8] J. Bohdansky, C.D. Croessmann and J. Linke, Proc. 14th Symp. on Fusion Technology, Avignon, 1986, p. 1063.

[9] J. Schou, in: Physical Processes of the Interaction of Fusion Plasmas with Solids, eds. W.O. Hofer and J. Roth (Academic Press, San Diego, 1995) pp. 177–216.